

# All-Raman-Amplified, 73 nm Seamless Band Transmission of 9 Tb/s Over 6000 km of Fiber

Lynn E. Nelson, *Senior Member, IEEE*, Xiang Zhou, *Senior Member, IEEE*, Benyuan Zhu, Man F. Yan, *Member, IEEE*, Patrick W. Wisk, and Peter D. Magill, *Member, IEEE*

**Abstract**—We report wavelength-division-multiplexed transmission of ninety 128-Gb/s polarization-multiplexed quadrature-phase-shift-keyed channels in a seamless 73 nm band over 60 × 100 km of ultra-large-area fiber. Co- and counter-pumped all-Raman amplification in the fiber spans, single-stage discrete Raman amplifiers, and broadband wavelength selective switch and channel equalizer were utilized to achieve optical signal-to-noise-ratio margin of more than 3 dB after 6000 km transmission of the 9 Tb/s capacity.

**Index Terms**—Optical fiber communication, optical fiber amplifiers, distributed Raman amplification.

## I. INTRODUCTION

AS CARRIERS attempt to continue to lower the cost-per-transmitted bit, research and development have concentrated on maximizing the benefits of coherent detection, in terms of obtaining the highest possible spectral efficiency. In order to increase capacity beyond the 100G systems with 88 to 96 wavelength-division-multiplexed (WDM) channels currently being deployed, multi-band transmission systems may be considered. Typical C+L-band systems with erbium-doped fiber amplifiers (EDFA) utilize ~70nm of bandwidth and require guard bands of 8 nm or more near 1565 nm, as recently reported in [1]. A seamless transmission band enabled by distributed Raman amplification avoids the band splitters and combiners required by systems with C+L EDFAs, thus simplifying the system configuration and potentially lowering cost. In addition, the reduced number of loss elements along the transmission link and distributed amplification in the fiber spans result in higher received optical signal-to-noise ratio (OSNR).

In the early 2000's, there were several demonstrations of ultra-wide, continuous single-band transmission including 10G submarine systems with seamless transmission bandwidths up to 80 nm using all-Raman amplification [2] or hybrid

Manuscript received August 5, 2013; revised November 6, 2013; accepted November 10, 2013. Date of publication November 20, 2013; date of current version January 8, 2014.

L. E. Nelson is with AT&T Labs, Middletown, NJ 07748 USA (e-mail: lenelson@att.com).

X. Zhou was with AT&T Labs, Middletown, NJ 07748 USA. He is now with Google, Inc., Mountain View, CA 94043 USA (e-mail: zhoux@ieee.org).

B. Zhu, M. F. Yan, and P. W. Wisk are with OFS Laboratories, Somerset, NJ 08873 USA (e-mail: bzhu@ofsoptics.com; mfy@ofsoptics.com; wisk@ofsoptics.com).

P. D. Magill was with AT&T Labs, Middletown, NJ 07748 USA. He is now with Silicon Lightwave Services, LLC., Newark, DE 19904 USA (e-mail: pmagill@alum.mit.edu).

Color versions of one or more of the figures in this letter are available online at <http://ieeexplore.ieee.org>.

Digital Object Identifier 10.1109/LPT.2013.2291399

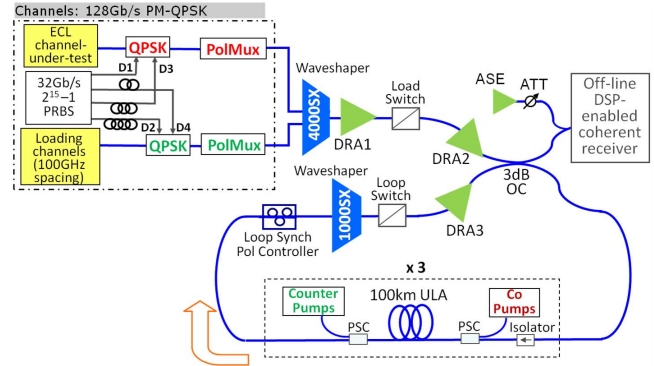


Fig. 1. Experimental setup: OC: optical coupler, PSC: pump-signal coupler. ATT: attenuator, ASE: amplified spontaneous emission.

Raman-EDFA repeaters [3]. For terrestrial applications, transmission of a 53nm continuous band with 2.5 Tbit/s ( $64 \times 42.7$  Gbit/s) capacity [4] and  $90 \times 42.7$  Gb/s in a 73nm band [5] were each demonstrated over 4000 km of fiber. Both [4] and [5] utilized non-zero dispersion-shifted fiber in the spans and in-line, Raman-pumped dispersion-compensating fiber (DCF) modules. Since those demonstrations, the adoption of digital coherent detection has obviated the need for inline dispersion compensation, thereby eliminating nonlinear impairments arising from Raman-pumped DCF in all-Raman-amplified systems. In addition, digital coherent systems' tolerance to dispersion lends flexibility in the design of the Raman fiber utilized in discrete Raman amplifiers.

Here we report transmission of ninety 128Gb/s polarization-multiplexed quadrature-phase-shift-keyed (PM-QPSK) channels in a seamless 73nm band over 60 × 100km of low-loss ultra-large-area (ULA) fiber. We employed all-Raman amplification in the fiber spans via co- and counter-pumping, along with simple, single-stage, counter-pumped discrete Raman amplifiers having noise figure as low as 6dB. Seamless wavelength-selective-switch functionality and equalization across the entire 73nm band were achieved by using commercial optical processors based on liquid-crystal-on-silicon. Although the experiment utilized 100GHz channel spacing, subsequent tests showed that transmission with 50GHz channel spacing, allowing 18Tb/s capacity in a single band, also could be feasible over similar distances.

## II. EXPERIMENTAL SETUP

Figure 1 shows a schematic of the experiment. A tunable external cavity laser (ECL) having less than 100kHz linewidth served as the channel-under-test and was

TABLE I  
DISCRETE RAMAN AMPLIFIER CHARACTERISTICS

	Raman Fiber				Avg Gain (dB)	Avg Noise Figure (dB)	Output Power (dBm)	Total Pump Power (dBm)	Number of pump wavelengths
	length (km)	A <sub>eff</sub> (sq μm)	1550nm atten (dB/km)	1550nm Dispersion (ps/nm/km)					
DRA1	9.1	26.3	0.39	12.1	14.8	6.5	18.5	29.8	5
DRA2	10.0	30.9	0.70	9.3	7.8	7.3	23.4	32.2	6
DRA3	7.0	26.3	0.39	12.1	15.0	6.0	21.5	31.1	5

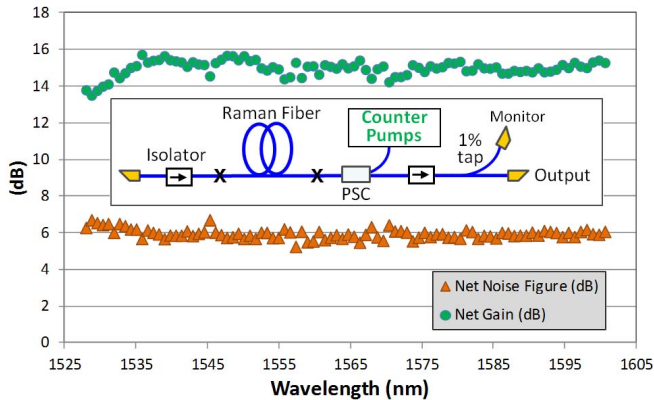


Fig. 2. Measured gain and noise figure of DRA3 in the loop. Inset shows the basic configuration of all three DRAs. (PSC: pump-signal coupler)

modulated with 32Gbaud QPSK via an I-Q modulator driven with  $2^{15} - 1$  pseudo-random-bit sequences (PRBS) with suitable inversion and delay to assure decorrelation of the I and Q data. The channel-under-test was then polarization multiplexed by splitting the signal, delaying one arm by 990 symbols, and recombining in a polarization beam combiner. A commercial  $1 \times 4$  Finisar Waveshaper WS4000SX was used as a wavelength selective switch to combine the channel-under-test with a band of 100GHz-spaced loading channels, which were separately PM-QPSK modulated (similar to the channel-under-test) to provide decorrelation of the WDM channels adjacent to the channel-under-test. The resulting signal was comprised of ninety 128Gb/s channels at 100GHz spacing in a continuous band from 1528.0nm to 1600.6nm.

Before the recirculating loop, the signals were boosted by two counter-pumped, single-stage discrete Raman amplifiers (DRA1 and DRA2), whose characteristics are listed in Table I and whose configuration is shown in the inset of Fig. 2. The WS4000SX was used to replace the loading channel with the channel-under-test as the ECL was tuned across the band, and to adjust the individual channel attenuations to flatten the spectrum at the output of DRA2 to within  $\pm 0.25$ dB, thereby providing a flat spectrum at the loop input.

The prototype ULA fiber had, at 1550nm,  $150 \mu\text{m}^2$  average  $A_{\text{eff}}$ , 21ps/nm/km dispersion, and 0.175dB/km average attenuation. The peak Raman gain efficiency was measured to be  $0.20/(W\text{-km})$  at 1455nm, where the fiber attenuation was 0.215dB/km. (Typical standard single-mode fiber has  $0.39/(W\text{-km})$  peak Raman gain efficiency [6] and attenuation of  $\sim 0.25$ dB/km near 1450nm.) Three ULA spans were configured for all-Raman amplification, as shown in Fig. 1, resulting in total span losses (fiber + components) of between

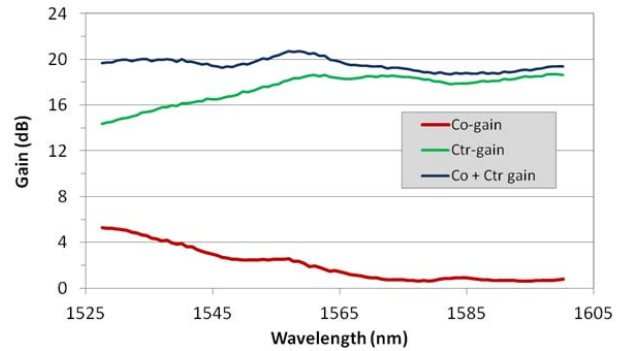


Fig. 3. Measured co-, counter-, and total gain for a typical 100km ULA fiber span.

19.1 and 20.1dB. For each span, counter-pumps at 1429, 1447, 1465, and 1495nm with 490, 427, 440, and 466mW, respectively, provide 14dB on-off Raman gain at the shorter wavelengths, and 19dB gain at the longer wavelengths. Co-pumps at 1425 and 1455nm with 365 and 114mW, respectively, provided a maximum of 5.8dB on-off Raman gain at the shortest wavelengths, with co-gain less than 1dB from 1570 to 1600nm, as shown in Fig. 3. The Raman-pumped ULA span noise figure, as defined in section IV(D) of [7], was estimated to be less than 16dB at all channel wavelengths, consistent with the low noise figure of all-Raman-amplified large- $A_{\text{eff}}$  fiber spans reported in prior publications (e.g. [6]). After the third span, the peak-to-peak variation of the channel powers was less than 5dB across the band. A loop-synchronous polarization controller to accurately emulate the polarization effects of a straight-line system was followed by a commercial Waveshaper WS1000SX for channel power equalization. The WS1000SX and WS4000SX each have an operating frequency range of 1527.4 nm to 1600.8 nm and optical transfer function [8] of 16 to 18GHz, compared to  $\sim 11$ GHz for a Waveshaper covering C-band only. DRA3 compensates for the attenuations of the WS1000SX, polarization controller, and loop components. As shown in Fig. 2, DRA3 had measured gain of 13.5 to 15.7dB and average noise figure of 6.0dB. Note that only DRA3 was optimized in terms of Raman fiber length; DRA2 used a new prototype fiber having larger  $A_{\text{eff}}$  but higher than expected loss. All three DRAs had positive dispersion at the signal wavelengths and thus provided no pre-dispersion compensation or inline dispersion compensation, as is optimal for coherent systems [9].

After 20 loops (6000km), each channel was independently received using a tunable optical filter with  $\sim 0.6$ nm  $-3$ dB bandwidth, followed by a polarization- and phase-diverse coherent receiver with balanced photodiodes having  $-3$ dB bandwidth of 40GHz. A four-channel real-time oscilloscope (with 80GSa/s and 33GHz bandwidth) performed the sampling and digitization function, followed by post-transmission offline digital signal processing of the captured data, as described in [10]. Errors were counted over  $1 \times 10^6$  bits of information for each WDM channel.

### III. TRANSMISSION RESULTS AND DISCUSSION

Optimization of the transmission system was carried out experimentally. First the launch power into the ULA spans

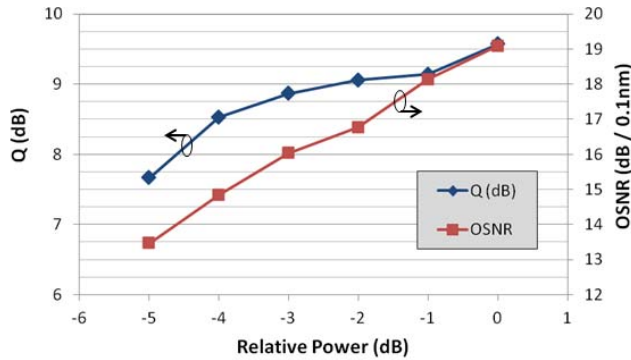


Fig. 4.  $20 \log(Q)$  and OSNR of the center channel after 6000km as a function of launch power, where 0dB relative power corresponds to  $-1.5\text{dBm/ch}$  at the input to each span.

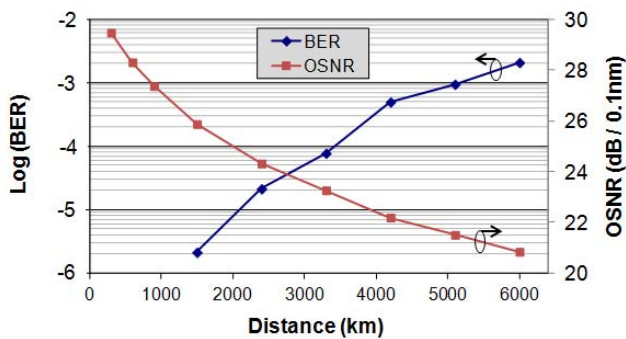


Fig. 5. Bit-error-ratio and OSNR of the center channel (at 1563.06nm) as a function of distance.

was set at  $+18.0\text{dBm}$  ( $-1.5\text{dBm/ch}$ ), which was the maximum available launch power due to the limited available pump power for DRA3 in the loop. Then the Raman pumps were adjusted to achieve transparency in each span and optimum flatness across the spectrum. In order to evaluate the launch power sensitivity without significantly affecting the spectral flatness, the launch power of the center channel (1563.05nm) and its ten nearest neighbors were attenuated in 1dB steps using the WS400SX, as the bit-error-ratio (BER) of the center channel was measured after 20 loops (6000km). Fig. 4 plots  $20\log(Q)$  (where  $Q$  is inferred from BER) and OSNR versus the relative launch power. Due to the complexities of the loop setup and per-channel equalization, one can see variations from a slope of 1 for the OSNR. For the interval from  $-5$  to  $-4\text{dB}$  relative power, the OSNR increases by 1.4dB, while  $Q$  increases by 0.9dB, thus indicating that the system was operating in a slightly nonlinear regime at the lowest channel power measured. However, Fig. 4 indicates that  $Q$  continues to improve with launch power, and the maximum available launch power provides the lowest BER at 6000km. Note that the optimal launch power for the ULA spans is significantly higher than the  $-6\text{dBm/ch}$  optimum span launch power for the experiment of Ref [5]. Fig. 5 plots the evolution of the bit-error-ratio and optical signal-to-noise ratio for the center channel (1563.05nm) as a function of transmission distance with launch power of  $-1.5\text{dBm/ch}$ . The optical spectrum after 6000km is shown in Fig. 6, where the peak-to-peak channel power variation was within 4dB.

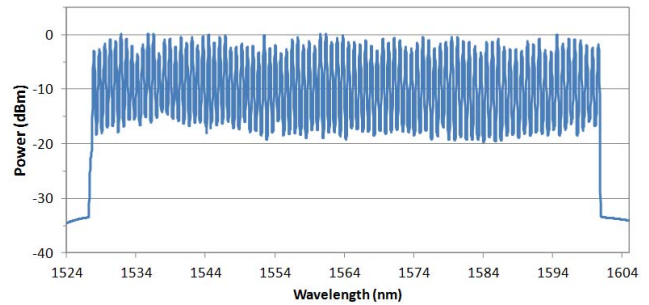


Fig. 6. Optical spectrum of the ninety 128Gb/s channels after 6000km transmission, measured with resolution bandwidth of 0.2nm.

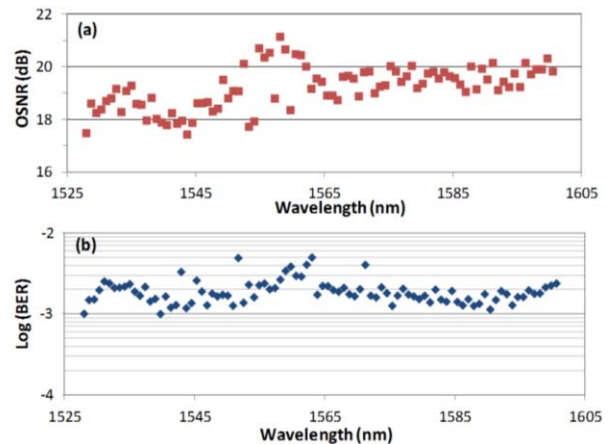


Fig. 7. (a) Measured OSNRs (in 0.1nm) and (b) bit-error-ratios for all 90 channels after 6000km transmission.

After 6000km transmission, the received OSNRs for the 90 channels ranged from 17.4 to 21.1dB (in 0.1nm), with average of 19.3dB (Fig 7a). The OSNRs had approximately 2dB of slope across the channels due to stimulated Raman scattering, which causes power transfer from the shorter wavelength channels to the longer wavelength channels. However, the co-pumping at 1425 and 1455nm mitigates the OSNR degradation of the short wavelengths. The average BER is  $2.0 \times 10^{-3}$  (as shown in Fig. 7b), and all 90 channels have BERs less than  $5 \times 10^{-3}$ , which is well below the threshold of  $2.4 \times 10^{-2}$  BER for 20% soft-decision forward error correction using quasi-cyclic low-density-parity-check code [11]. Figure 8a plots BER versus OSNR for the center channel (1563.05nm) for back-to-back and after 6000km transmission with addition of amplified spontaneous emission at the receiver (as shown in Fig. 1). Based on the least-squares fits, the OSNR penalty at  $2.0 \times 10^{-2}$  BER was 1.9dB. This penalty is quite close to the 1.76dB optimum nonlinear penalty derived in [12] from closed-form expressions for performance prediction of WDM PM-QPSK long-haul uncompensated transmission, thus indicating that the launch power was close to optimum. For this particular channel, the OSNR margin was nearly 7dB, and for channels with the lowest OSNR, the margin still would be more than 3.0dB.

Finally, to evaluate the possibility of 50GHz channel spacing, ten additional 100GHz-spaced channels were multiplexed with the channel-under-test before the PM-QPSK modulator

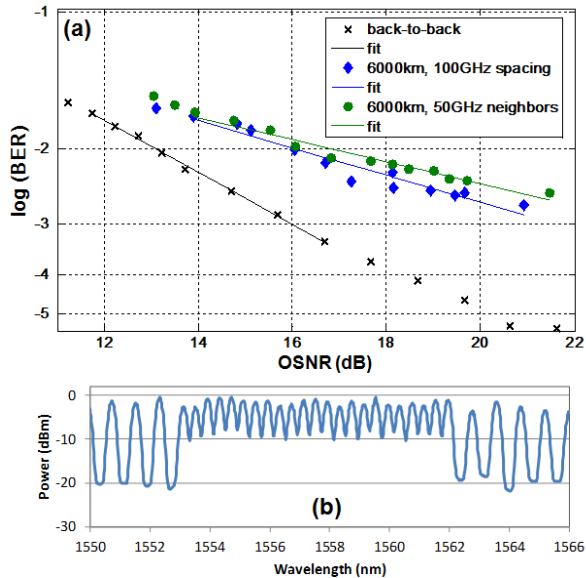


Fig. 8. (a) Comparison of BER vs OSNR performance of back-to-back, 1563.05nm channel with 100GHz channel spacing after 6000km, and 1557.77nm channel with 50GHz neighbors after 6000km. (b) Optical spectrum showing the 50GHz-spaced channels.

to create twenty-three 50GHz-spaced channels near the center of the band (which carried 100 channels in total). The per-channel power of the twenty-three 50GHz-spaced channels was set to be the same as the other 100GHz-spaced channels, so the nominal per-channel power was  $-2.0\text{dBm}$  (and close to the  $-1.5\text{dBm}$  per-channel power in the experiments with 90 channels at 100GHz spacing). The BER versus OSNR curve for the center 50GHz-spaced channel (at 1557.77nm, see Fig. 8b) was measured and is also plotted in Fig. 8a. Compared to the BER curve with 100GHz channel spacing, there is less than 1dB of additional OSNR penalty at  $2.0 \times 10^{-2}$  BER. Thus, we conclude that for these 100Gb/s PM-QPSK signals, due to the large  $A_{\text{eff}}$  and large dispersion of the ULA fiber, intra-channel nonlinearities are dominant over inter-channel nonlinearities, and the tighter channel spacing causes little additional nonlinear impairment. Given the more than 3dB margin for 100GHz spacing, and assuming that sufficiently powerful pumps would be available to provide inline discrete DRA and distributed Raman amplification supporting total launch powers of up to 21 dBm, transmission with 50GHz channel spacing (i.e. 18Tb/s) in a seamless 73nm band appears feasible over similar distances.

#### IV. CONCLUSION

In summary, we have demonstrated 6000km transmission of ninety 128Gb/s, 100GHz-spaced PM-QPSK signals in a

seamless 73nm band. The result was enabled by all-Raman amplification in 100km spans of ultra-large-area fiber and by low-noise-figure, single-stage discrete Raman amplifiers. Equalization of the spectrum was achieved using liquid-crystal-on-silicon optical processors capable of seamlessly covering the entire 73nm band. To our best knowledge,  $60 \times 100\text{km}$  is the longest transmission distance demonstrated for a  $>70\text{nm}$  seamless band of 100G channels. In addition, the OSNR margin of more than 3dB, coupled with less than 1dB additional OSNR penalty observed in tests with 50GHz-spaced neighbors compared to 100GHz spacing, indicate the potential for practical long-haul WDM systems carrying 100Gb/s channels on the 50GHz grid in a single seamless C+L band over distances of several thousand kilometers.

#### REFERENCES

- [1] M. Salsi, *et al.*, "31 Tb/s transmission over 7,200 km using 46 Gbaud PDM-8QAM with optimized error correcting code rate," in *Proc. 18th OECC/PS*, Kyoto, Japan, Jul. 2013, paper PD3-5.
- [2] N. Shimojoh, *et al.*, "2.4 Tbit/s WDM transmission over 7400 km using all Raman amplifier repeaters with 74 nm continuous single band," in *Proc. 27th ECOC*, vol. 6. Amsterdam, The Netherlands, Sep. 2001, pp. 8–9, paper PD.M.1.7.
- [3] D. G. Foursa, *et al.*, "2.56 Tbit/s ( $256 \times 10$  Gb/s) transmission over 11,000 km using hybrid Raman-EDFAs with 80 nm of continuous bandwidth," in *Proc. OFC Conf.*, Anaheim, CA, USA, Mar. 2002, pp. FC3-1–FC3-3, paper FC3.
- [4] A. H. Gnauck, *et al.*, "2.5 Tb/s ( $64 \times 42.7$  Gb/s) transmission over  $40 \times 100$  km NZDSF using RZ-DPSK format and all-Raman amplified spans," in *Proc. OFC Conf.*, Anaheim, CA, USA, Mar. 2002, pp. FC2-1–FC2-3, paper FC2.
- [5] B. Zhu, *et al.*, "Broad bandwidth seamless transmission of 3.56 Tbit/s over  $40 \times 100$  km of NZDF fibre using CSRZ-DPSK format," *Electron. Lett.*, vol. 39, no. 21, pp. 1528–1530, Oct. 2003.
- [6] L. Nelson and B. Zhu, "40Gb/s Raman-amplified transmission," in *Raman Amplifiers for Telecommunications*, vol. 2. New York, NY, USA: Springer-Verlag, 2004, pp. 673–721.
- [7] J. Bromage, "Raman amplification for fiber communications systems," *J. Lightw. Technol.*, vol. 22, no. 1, pp. 79–93, Jan. 2004.
- [8] C. Pulikkaseril, L. A. Stewart, M. A. F. Roelens, G. W. Baxter, S. Poole, and S. Frisken, "Spectral modeling of channel band shapes in wavelength selective switches," *Opt. Express*, vol. 19, no. 9, pp. 8458–8470, Apr. 2011.
- [9] V. Curri, P. Poggiolini, A. Carena, and F. Forghieri, "Dispersion compensation and mitigation of non-linear effects in 111 Gb/s WDM coherent PM-QPSK systems," *IEEE Photon. Technol. Lett.*, vol. 20, no. 17, pp. 1473–1475, Sep. 1, 2008.
- [10] L. E. Nelson, X. Zhou, N. Mac Suibhne, A. D. Ellis, and P. Magill, "Experimental comparison of coherent polarization-switched QPSK to polarization-multiplexed QPSK for  $10 \times 100$  km WDM transmission," *Opt. Express*, vol. 19, no. 11, pp. 10849–10856, May 2011.
- [11] D. Chang, *et al.*, "FPGA verification of a single QC-LDPC code for 100 Gb/s optical systems without error floor down to BER of  $10^{-15}$ ," in *Proc. OFC/NFOEC*, Los Angeles, CA, USA, Mar. 2011, paper OTuN2.
- [12] G. Bosco, *et al.*, "Performance prediction for WDM PM-QPSK transmission over uncompensated links," in *Proc. OFC/NFOEC*, Los Angeles, CA, USA, Mar. 2011, paper OTh07.